

## **General Disclaimer**

### **One or more of the Following Statements may affect this Document**

- This document has been reproduced from the best copy furnished by the organizational source. It is being released in the interest of making available as much information as possible.
- This document may contain data, which exceeds the sheet parameters. It was furnished in this condition by the organizational source and is the best copy available.
- This document may contain tone-on-tone or color graphs, charts and/or pictures, which have been reproduced in black and white.
- This document is paginated as submitted by the original source.
- Portions of this document are not fully legible due to the historical nature of some of the material. However, it is the best reproduction available from the original submission.

A STUDY OF  
ATMOSPHERE-IONOSPHERE-MAGNETOSPHERE  
COUPLING

(NASA-CR-168972) A STUDY OF  
ATMOSPHERE-IONOSPHERE-MAGNETOSPHERE COUPLING  
Final Report (Utah State Univ.) 36 p  
HC A03/MF A01 CSCI 04A

N82-25678

Unclas  
G3/46 27920

NASA Grant NAG5-121

Final Report

October 1, 1980 - December 31, 1981

Submitted by:

W. J. Raitt, Principal Investigator  
J. L. Parish, Co-Investigator  
Center for Atmospheric & Space Sciences  
UMC 34  
Utah State University  
Logan, Utah 84322

May, 1982



## 1. Introduction

Early work of Axford and Hines (1961) and Dungey (1961) on the configuration of the earth's distant geomagnetic field due to the interaction of the solar wind and the earth's geomagnetic field led to the now generally accepted view of the gross features of the magnetosphere. The effect of the interaction is to generate current systems which result in the earth's geomagnetic field on the sunward side being compressed and on the anti-sunward side being drawn out into a long tail-like structure. The magnetic field lines which form the tail of the magnetosphere originate from the polar regions of the earth's surface. One result of the extended tail of the magnetosphere is that there will be a continual plasma pressure gradient away from the earth parallel to the magnetic field lines between the relatively dense ionospheric plasma at about 300 km altitude and the distant geomagnetic tail.

Initial studies of the effects of plasma density gradients on the diffusion dominated regions of the ionosphere had concentrated on applying plasma transport equations to solve for the case of the diffusive equilibrium distribution of multi-ion species (cf. Mange, 1960). In this case, the pressure gradient existing between the F-region peak and higher altitudes results in the ions distributing themselves such that the polarization electric field set up by the pressure gradient is just balanced by the gravitational force on the ions. Under these circumstances the outward flux of ions is zero. When the concept of open or extended field lines became accepted, it was realized that the possibility existed for ions to continuously flow out from the earth into distant regions of the magnetosphere linked by geomagnetic field lines to the polar ionosphere. This condition is one of the solutions of the ion density distribution under diffusion dominated conditions and is known as 'dynamic

equilibrium' as opposed to 'diffusive equilibrium' discussed earlier. Both types of equilibrium represent steady state solutions to the plasma transport equations resulting in the requirement that the outward flux is a constant, zero in the case of diffusive equilibrium and some finite value in the case of dynamic equilibrium (Banks and Kockarts, 1973; Bauer, 1973). Boundary conditions on the rate of production of the outflowing ions and Coulomb collisions with stationary ions result in an upper limit to the outward flux. The most dramatic ionospheric effect of dynamic equilibrium is to produce a marked reduction in ion density of the outflowing species compared with the diffusive equilibrium situation. For a single ion species in its parent neutral gas, with electron, ion and neutral temperatures equal, the scale height is decreased by a factor of two for the change from diffusive to dynamic equilibrium.

For a mixture of light and heavy ions such as  $H^+$  and  $O^+$ , detailed solutions of the plasma transport equations show that the gravitational attraction on the heavier  $O^+$  ion is such that the polarization electric field is not sufficient to permit the dynamic equilibrium condition and the ions form a diffusive equilibrium altitude-density profile. However,  $H^+$  is light enough that once the inhibiting effect of  $H^+-O^+$  collisions is reduced as the  $O^+$  density falls off, the polarization electric field can drive the ions into a continuous outflow parallel to the geomagnetic field (Banks and Holzer, 1968). This outflow of light ions from the polar regions of the earth's ionosphere was termed the polar wind by Axford. Further studies (Banks and Holzer, 1969a, 1969b) have shown that  $He^+$  is also light enough to flow out along open geomagnetic field lines, although the characteristics of the outflow differ considerably from that of  $H^+$ .

As the polar wind ions increase their outflow velocity when they escape the effects of Coulomb collisions with  $O^+$ , the conventional plasma transport equations eventually become invalid due to the transition from collision dominated motion to collisionless motion. To accommodate the collisionless region, kinetic models of the polar wind have been developed by Dessler and Cloutier (1969) and by Lemaire and Scherer (1970, 1971, 1972). Comparisons between the hydrodynamic and kinetic models of the collisionless polar wind have shown that a good match occurs between the two techniques (Holzer et al, 1971).

The studies of both the diffusive and dynamic equilibrium distribution of ion density with altitude which have been published are of steady state conditions. At present, no detailed studies of the time dependent nature of the outflow have been made, although some speculations on the characteristics of a shock front propagating along a suddenly depleted flux tube have been made (Banks et al, 1971).

It is apparent that this outflow of plasma will provide a source of magnetospheric plasma in the distant magnetospheric tail with its origin in the plasma generated in the polar regions by ionization of the earth's neutral atmosphere by solar ultraviolet light in the sunlit pole and by particle ionization over the whole of the polar cap but concentrated in the auroral regions. The outflowing plasma into the magnetospheric tail is generated as a relatively cool thermal plasma. However, recent studies have shown that quite drastic modifications occur to the distribution functions of both the ions and electrons are predicted to occur as the plasma flows away from its source region in the ionosphere to great distances along the geomagnetic field lines.

As was mentioned above, the ultimate source of the polar wind is the polar ionospheric plasma which has a peak density at around 300 km altitude. The source of  $H^+$  to form the main element of polar wind is the accidentally resonant charge exchange reaction



Thus, the amount of  $H^+$  available to flow away from the earth is directly controlled by the ambient density of  $O^+$  ions in the topside ionosphere. Recent studies of the distribution of ion densities over the polar cap as a function of position and time have shown that the  $O^+$  density is by no means uniform. Hence, different flux tubes will have different initial plasma pressures to drive the polar wind, resulting in varying outward fluxes. The large variability of  $O^+$  density is a result of mapping the convection electric field about the magnetic pole which rotates diurnally about the geographic pole in the geographic reference frame (Sojka et al, 1979, 1981a, 1981b).

The source of  $He^+$  ions flowing away from the earth's ionosphere is less variable than the  $H^+$  source, since it is produced primarily by chemical balance between the photoionization of He and charge exchange between  $He^+$  and the molecules  $O_2$  and  $N_2$ . However, local heating of the neutral atmosphere by plasma drift or by particle precipitation will increase the loss processes for  $He^+$  in localized regions. The sources and Coulomb collision processes in the topside ionosphere for the  $H^+$  and  $He^+$  ions result in a flux limited outflow having values as large as  $3 \times 10^8 \text{ cm}^{-2} \text{ sec}^{-1}$  for  $H^+$  ions and  $2 \times 10^7 \text{ cm}^{-2} \text{ sec}^{-1}$  for  $He^+$  ions.

The fate of the outflowing plasma when it reaches the magnetosphere has been studied theoretically by Schunk & Watkins (1981, 1982) who have shown that marked anisotropies are predicted to develop as the polar wind plasma

flows away from the earth. These anisotropies may be unstable and lead to wave-particle instabilities either from the flowing plasma itself or from an interaction with the environment through which the plasma is flowing.

At present measurements of the low energy ion component of the magnetospheric plasma have shown that unusual pitch angle distributions are not uncommon (Horowitz et al, 1981) and that a significant population of ions with energies around 10 eV and higher exists (Chappell, 1980). Unfortunately instrumental problems associated with vehicle charging often preclude ion measurements below 10 eV, and apart from an experiment flown on the ESA GEOS spacecraft, there have been no instruments flown which concentrate solely on measuring the detailed distribution function of the low energy electron population in the magnetospheric plasma.

In this study we had planned to use low energy ion distribution measurements from the ISEE spacecraft to guide the theoretical interpretation of processes occurring as the polar wind flows into the magnetosphere. However, we only received an undocumented data tape near the end of the nominal period of performance. Consequently we started developing a new theoretical approach to predict the properties of low energy plasma in the magnetosphere. These studies were directed to studying the effects of wave-particle interactions involving the concept of plasmons and thereby drawing on quantum mechanical formulation for the processes occurring and also to study bulk energization of the low energy plasma through the concept of the energy momentum tensor for the plasma and its electromagnetic environment.

## 2. Comparison of Macroscopic and Microscopic Approach

The dynamical behavior of high energy plasma may be determined using single particle equations. For low energy plasma, collisional effects are important and one must use a fluid picture. This leads to a macroscopic view considering mass, momentum and energy flows. These flows are related to macroscopic gradients by diffusion coefficients which are determined by microscopic processes such as wave-particle scattering. In addition, the effects of the macroscopic flows are related to measurements through distribution functions which are microscopic quantities. We, therefore, took a two - pronged approach, both macroscopic and microscopic, to study the interaction of flowing plasma populations.

### 2.2 Macroscopic Modeling Technique

The conventional fluid equations are differential equations which are difficult to use with measured data because of noise in the measurements which can lead to erroneous derivatives. We use, instead, the general principle that a differential equation can be formulated as an integral equation (Ince, 1926; Chandrasekhar, 1961). Thus, instead of working from the force equation, that is, the differential form of the momentum balance equation, we considered the momentum flux directly, that is, the integral form of the momentum balance equation. Further details of the technique are contained in a submitted paper entitled "Energy and Momentum Flow in Electromagnetic Fields and Plasma".

By solving the integral form of the momentum balance equation, we determined the momentum flow with several advantages over solutions of the differential equation.



(1) Our approach is conceptualized differently and more systematically than the differential approach. We look at the energy-momentum tensor, specifically at the components of this tensor which are the momentum fluxes. This is conceptually different because now we realize that fields as well as particles may carry momentum. The approach is more systematic because we can easily handle momentum flow of fields and particles as well as momentum flow due to friction. That is, it is easier to identify the mechanisms which carry momentum and understand the contribution from each.

(2) Differential equations are most commonly written in a given coordinate system for instance spherical coordinates. Our integral equations are written in a general coordinate system whose geometry is determined by the metric of the coordinate space. This along with General Relativistic notation greatly simplifies the algebra used to derive results. When our algebra is finished, we can apply our results in any coordinate system by choosing the metric for rectangular, spherical, cylindrical or any other coordinate space.

(3) Data can be used without generating large relative errors inherent in numerical differentiation.

(4) The method is general and basic and can be used on almost any data. With proper statistical handling it can be applied to turbulent data.

These four advantages to balancing the momentum are also present in the integral form of energy balance. Balancing the energy is more difficult than momentum balance because we must use the thermodynamic characteristics of the plasma which are not entirely known.

Limited use has been made of this method by Yeh et. al. (1981) who derived a theoretical expression for the energy coupling of the solar wind and the magnetosphere. They looked at the spacial transport in the magnetic field by using part of the energy momentum tensor. Cowley (1980) has made a study of magnetospheric energy transport where he considered the balance between Joule heating and the spacial transport of energy by the electromagnetic field. Spacial energy flow in the magnetic fields can flow into Joule heating, but it can also go into internal energy of the plasma or be used to accelerate the plasma. A large scale energy source such as low order multipoles generated by currents in the earth may provide a 'production range' energy source for MHD turbulence. Cowley (1980) writes down (an incomplete set) the momentum balance equations but does not make use of them.

We have formalized this work, introducing a notation which is brief and convenient and to more fully utilize the power of the macroscopic approach.

Even though most of the basic ideas are contained in classical electromagnetic, Stratton (1941) or J.D. Jackson (1962), the most complete discussion, however, occurs in General Relativity, Weinberg (1972). General Relativity operates in 4-space with a given metric for this space resulting in a notation which is brief and manageable. By choosing the metric to be rectangular, spherical or cylindrical we can readily operate in any of these coordinate systems.

The energy momentum tensor for a perfect fluid in a magnetic field is

$$T^{\alpha\beta} = p(\delta^{\alpha\beta} + u^{\alpha}u^{\beta}) + \rho u^{\alpha}u^{\beta}$$

$$+ (F^{\alpha}_{\zeta} F^{\beta\zeta} - 1/4 \delta^{\alpha\beta} F^{\nu\mu} F_{\nu\mu})$$

$p$  is the proper pressure; here  $u^i = v^i/\gamma$ ;  $v^i$  is the  $i$ th component of proper velocity and  $u^0$  is  $\gamma = (1 - v^2)^{1/2}$ ;  $\alpha, \beta = (0, 1, 2, 3)$ ;  $i = (1, 2, 3)$  and velocities have been normalized to the speed of light.

This is the integral form of the momentum and energy balance equation, integrating  $T^{\alpha\beta}$  over 4 - space produces a constant. The differential form of the MHD equations are contained in  $T^{\alpha\beta}$  by taking the 4 - divergence and equating it to zero,  $T^{\alpha\beta}_{;\beta} = 0$ .

In the paper mentioned above we have been careful to take limits in the correct order, which is not always done, Misner et. al. (1973). We took the  $\gamma \rightarrow 1$  limit after taking the derivatives. In this way we derived from this equation the hydrodynamic equations of Landau and Lifshitz (1959), and the magnetohydrodynamic equations of Lundquist (1952).

At the present stage of development, we have formulated the situation for an ideal fluid in an electromagnetic field (Parish & Raitt, Energy and momentum Flow in Electromagnetic Fields and Plasma, Planetary and Space Sciences, submitted, 1981a). The next step is to include a viscous term in the energy momentum tensor allowing us to consider the momentum and energy flow due to viscosity in a dissipative fluid in an electromagnetic field.

Satellite data requires special care in use, beyond proper data reduction to remove instrument errors, even ideal measurements from a satellite are one point in space and time (ISEE A & B make two point measurements but the arguments are the same). If the velocity field, the spacecraft is measuring, var-

ies slowly in time and in space, then the measurement made represents the average velocity at that point. If, however, the velocity field is strongly turbulent, the velocity field is a random variable and the single measurement made could differ significantly from the actual average.

In addition to applying our method to quiet areas, we have set up to make a proper statistical analysis of data in turbulent areas. This involves finding the correlation length and determining the correlation between velocity components, magnetic field components and between velocity and magnetic field components. Because of the bilinear nature of the terms in the energy momentum tensor which may be evaluated from two point correlation functions, and because the tensor deals with momentum and energy flows, it is necessary to investigate the relation of our new procedure to older turbulent transport theory of Kraichnan (1976a,b), Kraichnan and Nagrajan (1967) and Fyfe et. al. (1977). Strong turbulence is non-linear and the large scales of planetary environments make satellite measurements of turbulence unique and valuable. This application holds the possibility of testing and refining the MHD turbulence theories.

### 2.3 Microscopic Modeling Technique

Following the observations of outwardly accelerated ions possibly generated by the mechanism which inwardly accelerates auroral electrons, we worked on a model which studies the interaction of oppositely streaming plasmas to see if the heating observed by various workers (cf. Chappell (1980), Chappell et al. (1980)) referred to earlier is predicted. Our model predicts the distribution of the resulting plasma for direct comparison with the distributions measured in situ by magnetosphere satellites such as the ISEE-1 low energy

plasma analyzer or the ESA GEOS experiment which also has low energy plasma analysis included in the payload.

There are two commonly used methods of handling a plasma numerically when it is considered as a collection of individual particles rather than a fluid. Either one follows the exact orbits of the particles resulting in the tracking of  $3N$  coordinate points for  $N$  particles or one uses a statistical or Monte Carlo method and group the particles into velocity bins by means of a velocity distribution function and then uses the Vlasov equation. The former approach has the disadvantage of needing very large computer resources and also generating so many instabilities that they are hard to characterize. The latter approach uses less computer resources, but tends to be too restrictive in the solutions attainable. The approach we have adopted falls between the two commonly used methods discussed above. This technique allows a variety of instabilities and non-linearities to be handled in a controlled manner and the effective wave-particle interactions occurring to be quantified.

At present, we have limited ourselves to Langmuir wave-particle interactions to improve our understanding of the model. Our initial experience has indicated that this modeling approach will require less computer resources than other methods and will also be readily extendable to include other forms of plasma wave instability than the Langmuir waves we are currently studying.

Wave-particle interactions dominate binary collisions in the magnetosphere and the approach we are developing is a new method of studying space plasmas and involves the application of Quantum Statistical Mechanics to these plasma interactions. The general basis for this technique has been described by Harris (1969), Pines (1962), Pines and Schrieffer (1962), Abrikosov, Gor-

kov, Dzyaloshinski (1963), Fetter and Waleska (1971) and references therein.

The phenomena we are investigating are classical with no quantum effects, and it is possible to develop this formulation along classical lines (See Martin, Siggia and Rose (1973); Krommes (1979); Rose (1979); Mishima, Petrozky, Suzuki (1979)). This classical formulation, however, is in early stages of development while the quantum mechanical theory is highly developed and so we take advantage of this by using the quantum mechanical treatment, in the classical limit  $\hbar \rightarrow 0$ . This theory is very powerful, and is well suited to handle the large number of degrees of freedom and the nonlinearities inherent in wave-particle interactions.

Non - linearity in a plasma may be put into two categories. The first is an effective increase in the mass of the particles in the plasma due to the electromagnetic interactions of the charged particle with other particles. Correcting for this effective mass is known as 'mass renormalization'. The second category is the correction of the electromagnetic force between two charges due to other charges being present; this is known as 'vertex renormalization'. Mass and vertex renormalization are not independent and plasmas are usually treated using 'vertex renormalization'. This allows us to account, for example, for the effects of a large amplitude wave on the plasma through which it propagates, which in turn affects the wave itself.

We start with the Schrodinger equation. Since the Vlasov equation may be derived from this equation (see van Roos (1960), Saenz (1957), Takabayasi (1954), Ross and Kirkwood (1957), Dahler (1959), Klimontovich (1958)), all solutions to the Vlasov equation are contained in our approach. The Schrodinger equation is first order in time and along with initial conditions will give

the time development of a quantum mechanical system. The system is described by a wave function which gives the states of the particles and waves which make up the system.

In formulating the plasma processes we second quantize, that is, we consider the electrostatic or electromagnetic field as being made up of particles. In the case of Langmuir waves, these particles are called plasmons.

We represent the state of the electrons or plasmons as

$$\Psi = \prod_r N(r) \phi_r$$

where  $\phi_r$  is the state of one particle, characterized by its momentum and energy and  $N(r)$  is the occupation number or number of particles in the state  $\phi_r$ . We use Fermi's Golden Rule to find the change in the occupation number of a state  $r$ . The occupation number is the number of electrons or the number of plasmons in a state  $p_r$ .

$$\partial N(r)/\partial t = 2\pi/\hbar \sum_s |M_{rs}|^2 \rho_s \quad (1)$$

$\rho_s$  is the density of states around state  $s$ .  $|M_{rs}|^2$  is the transition probability of a transition from a state  $s$  to a state  $r$ .

$N$  can represent the number of electrons or the number of plasmons in state  $r$ . For discussion, we let  $N(r)$  be the number of electrons in state  $r$ , equations similar to those are deriving hold for plasmons. We now expand the right hand side of (1) into two terms. The first term represents the transitions which put an electron into state  $r$  and a second term which represents an electron in state  $r$  making a transition out of state  $r$  into any other state.

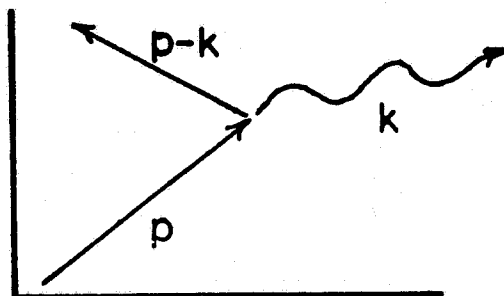
$$\frac{\partial N(r)}{\partial t} = (\text{transitions per unit time into state } r)$$

$\partial t$

$$- (\text{transitions per unit time out of state } r)$$

The number of transitions per unit time into state  $r$  from another state  $s$ , is the probability that the electrons will make the transition from  $s$  to  $r$  times the probability that there is an electron in state  $s$  times the probability that state  $r$  is empty. State  $r$  must be empty for electrons since they are Fermions and each state cannot hold more than one. In our case, an electron makes a transition into or out of a state by emitting or absorbing a plasmon.

We may represent a single transition with a Feynmann diagram. For discussion, we consider only an electron in state  $s$  emitting a plasmon into a state  $t$  causing the electron to go into state  $r$ . During the transition momentum is conserved, and we use the momentum to label the states; state  $s$  is labeled by  $p$ , state  $t$  is labeled by  $k$  and state  $r$  is labeled by  $p-k$ . Time increases upward in this diagram:



The point at which the transition takes place is called a vertex. We see that associated with each vertex is the transition probability  $|M_{rs}|^2$ .  $|M_{rs}|^2$  is the probability that an electron emits a plasmon. The transition probabilities  $|M_{rs}|^2$  are given by Harris (1969) or may be derived along the lines given by Bardeen and Pines (1955). The transition probabilities given by



Harris are for a bare vertex. We renormalize the vertex, which allows us to account for close Coulomb collisions. The long-range interactions, outside the Debye sphere, are represented by the plasmons. If  $k$  is negative, the process just described is the absorption of a plasmon by an electron. We now see that by generalizing this procedure to include all possible transitions, we can calculate the change in electron and plasmon distributions. We start with an initial distribution of electrons and plasmons and let the computer keep track of all transitions and changes in the distribution functions.

Up to now we have considered two beams streaming toward each other. This may, for instance, simulate two beams coming from conjugate hemispheres into the equatorial plane just outside the plasmasphere. We consider only the interactions of the streaming electrons and each beam is assumed to have a neutralizing ion background with which it has no interactions. The two beams are assumed to be symmetric; that is, they have the same density, average flow velocity and temperature.

We can obtain both the real and imaginary frequency; that is, the energy and decay rate of plasmons from this analysis. However, initially, we calculated only the imaginary part of the frequency. The real part of the frequency we find from standard linear analysis, singling out Langumir waves. This allows us to confine our attention to only one set of waves and look at their production and damping without the added complication of many different modes.

The electron distribution was quantized into momentum spectrum steps of  $10^7 \text{ cm}^{-1}$  and used 600 levels in the simulation. The simulation was one dimensional with 300 positive momentum steps and 300 negative momentum steps. In each momentum bin, the number of electrons is  $N_e(p)$ .

We started with two Maxwellians streaming toward each other with velocity corresponding to an energy of 10 eV, measured in units of  $m_e v^2/2$  relative to an inertial frame,  $m_e$  is the mass of an electron. The temperature of each beam was 4 eV, and its density was 100 electrons/cc. The plasma frequency was  $\omega_p = .1$  MHz, and the time step was  $\omega_p/10$  or  $10^{-6}$  second. The initial distribution is shown in Figure 1. We ran our simulation for 19 time steps, and the final electron distribution is shown in Figure 2. These figure show the two Maxwellians overlapping and the quantization of putting  $N_e$  electrons into a bin.

As a check on the validity of our simulation, we continually calculated the total electron density which, electrons being Fermions, should remain constant. We see from Figure 3 that the total number of electrons was conserved by the simulation at each time step.

Since we treat the plasma waves as particles or plasmons, we have quantized their electric field. The plasmon distribution was quantized into momentum bins of size  $10^{-3} \text{ cm}^{-1}$ . The number of plasmons in bin  $p$  is  $N_\lambda(p)$ . The simulation was started without plasmons and after 19 time steps, the plasmon distribution developed to that shown in Figure 4. We see that eight bins, four with positive momenta and four negative bins, a reflection of the positive ones through zero, contain plasmons. This shows the quantization of the waves as a certain number of plasmons contained in a bin.

The plasmons are bosons and their number is not conserved in the calculation. Indeed, we have started with a plasma with no waves in it, and the simulation has created waves or plasmons. The time behavior of the total plasmon density is shown in Figure 5. We see that the time behavior is very erratic

in the first few steps of generating the plasmons.

These plasmons were generated by spontaneous emission. As the number of plasmons increases with time, we expect stimulated emissions to become important. The simulation allows the plasmons to alter the distribution of the electrons. The altered distribution is used in the next timestep to generate plasmons. In this way the plasmons present in the plasma effect their own distribution. We never reached sufficient plasmon density for stimulated emission, in this case of only 19 timesteps, the plasmon levels were not large enough to alter the electron distribution (see Figures 1 and 2).

In order to study the lifetime of the Langmuir waves corresponding to the decay of plasmons used in the model, we calculated the damping decrement given by

$$\gamma = \frac{1}{2N_{\lambda}(p)} \frac{\partial N_{\lambda}(p)}{\partial t}$$

at each timestep. The initial damping decrement is shown in Figure 6. There are no plasmons at the first timestep and so  $\gamma$  was calculated from Harris (4.17) and corresponds to the Landau damping decrement.

After 19 timestep, the damping decrement is shown in Figure 7. We see that the plasmons generated are heavily damped as shown by the 'spikes' greatly exceeding the initial Landau damping.

We have shown that by using computer techniques on an old formalism that we can obtain reasonable results. We have produced waves from two counter streaming electron beams. We have followed the time development of these waves, and we have calculated the damping decrement. We have prepared this new method to rederive the classical results of calculations and numerical simula-

tion for the limits on stability, wave spectrum and damping.

We set up the software to continue the development of this model and use a combination of the particle distribution functions and the wave fields measured directly by magnetospheric satellites to test the predictions of the model and, thereby, establish the validity of this new theoretical approach to modeling the dynamics of space plasmas.

This method has been enormously successful in Quantum Electrodynamics in describing energy shifts (Lamb shift) and in Quantum Statistical Mechanics applied to metals and super - conductivity. This is a very powerful method to handle the non - linearities which arise in particle - wave and wave - wave interactions. However, use of this technique in space plasma physics is in its infancy. The theory is readily applicable to a tenuous plasma, to a plasma containing a magnetic field, to a plasma containing large amplitude waves, to name just a few areas of research which will benefit from the research.

### 3. Suggestions for Future Work

#### 3.1 Foundation for Future Work

##### 3.1.1 Macroscopic

The work done on both the microscopic and macroscopic theory have layed the foundation for future studies.

The macroscopic study is enormously powerful and particularly well-suited to study the large scale measurements of Space Physics. This approach has been touched on but never used to its full extent. There seems to be two beliefs in Space Physics; firstly, that the macroscopic approach is unconventional and therefore inappropriate; and secondly, that all that is involved is to use the energy momentum tensor. This last belief shows a lack of understanding that there are several other aspects as discussed earlier.

The macroscopic approach also leads us naturally into consideration of MHD turbulence. There is an enormous turbulence literature in the Journal of Fluid Mechanics and Physics of Fluids. These studies consider both hydrodynamical and magnetohydrodynamical turbulence and consist mostly of computer simulations. Turbulence depends on a parameter, the Reynolds number, which depends linearly on the size of the system. Turbulence is non-linear and Space Physics measurements are the only ones which have been made on a large enough system that internal turbulence measurements are available to test the computer simulations.

The high time resolution magnetic field and particle distribution measurements now being made on a number of geophysical spacecraft are particularly well suited to a macroscopic study. With these we should be able to look at the turbulence in the magnetic and velocity fields and compare results to the

computer simulations.

### 3.1.2 Microscopic

Work on the macroscopic is now suspended because of lack of funding; on the other hand, the microscopic theory which was designed to describe the polar wind is now being used to analyze the beam plasma experiments performed both in vacuum chambers and aboard the Space Shuttle. The microscopic theory applied to the magnetosphere requires wave data and particle data from current magnetospheric satellites, at present this work is also suspended due to lack of funding. However, we feel that the method holds promise for being able to model some of the wave particle interactions in a simpler manner and over a wider range of wave modes than is possible with quasi-linear or non-linear plasma theory.

#### 4. MATERIAL PRESENTED UNDER GRANT

Parish, J.L. and W.J. Raitt, Energy and momentum flow in electromagnetic fields and plasmas, Planetary and Space Sciences, submitted, 1981a.

Parish, J.L. and W.J. Raitt, Momentum and energy flow in the magnetosphere, AGU Fall Meeting, 1981b.

Parish, J.L. and W.J. Raitt, Modeling wave-particle interactions in space plasmas using quantum-mechanical techniques, Yosemite '82: Origins of Plasmas and Electric Fields Conference, 1982a.

Parish, J.L. and W.J. Raitt, Space plasma wave-particle interactions using quantum mechanical techniques, 1982b, USU Report.

## 5. BIBLIOGRAPHY

- Abrikosov, A.A., L.P. Gorkov and I.E. Dzyaloshinski, Methods of quantum field theory in statistical physics, Dover, New York, 1963.
- Axford, W.I. and C.O. Hines, A unifying theory of high-latitude geophysical phenomena and geomagnetic storms, Can. J. Phys., 39, 1433-1464, 1961.
- Banks, P.M. and T.E. Holzer, The polar wind, J. geophys. Res., 73, 6846-6854, 1968.
- Banks, P.M. and T.E. Holzer, Features of plasma transport in the upper atmosphere, J. Geophys. Res., 74, 6304-6316, 1969a.
- Banks, P.M. and T.E. Holzer, High-latitude plasma transport: The polar wind, J. Geophys. Res., 74, 6317-6332, 1969b.
- Banks, P.M. and G. Kockarts, Aeronomy, (Part B), Academic Press, New York, 1973.
- Banks, P.M., A.F. Nagy and W.I. Axford, Dynamical behavior of thermal protons in the mid-latitude ionosphere and magnetosphere, Planet. Space Sci., 19, 1053-1067, 1971.
- Bardeen, J. and Pines, D. Electron-Phonon Interactions in Metals, Phys. Rev. 99, 1140-1150, 1955.
- Bauer, S.J., Physics of Planetary Ionospheres, Springer-Verlag, Berlin-Heidelberg, 1973.
- Baughar, C.R., C.R. Chappell, J.L. Horwitz, E.G. Shelley and D.T. Young, Initial thermal plasma observations from ISEE 1, Geophys. Res. Lett.,



7, 657-660, 1980.

Cameron, A.G.W., Space Plasma Physics: The study of solar-system plasmas, vol. 1, National Academy of Sciences, Washington, D.C., 1978.

Chandrasekhar, S., Hydrodynamic and hydromagnetic instability, Clarendon Press, London, 1961.

Chappell, C.R., C.R. Baugher and J.L. Horwitz, New advances in thermal plasma research, submitted to Reviews of Geophysics and Space Physics, 1980.

Chappell, C.R., Low energy particles in the magnetosphere, Cospar background paper: current and future state of space science, 1980.

Dahler, J.S., Transport phenomena in a fluid composed of diatomic molecules, J. Chem. Phys., 30, 1447-1475, 1959.

Dessler, A.J. and P.A. Cloutier, Discussion of the letter by Peter M. Banks and Thomas E. Holzer, "The polar wind", J. Geophys. Res., 74, 3730-3733, 1969.

Dungey, J.W., Interplanetary magnetic field and the auroral zones, Phys. Rev. Letters, 6, 47-48, 1961.

Fetter, A.L. and J.D. Walecka, Quantum Theory of Many-Particle Systems, McGraw-Hill, New York, 1971.

Harris, E.N., Advances in Plasma Physics, vol. III, ed. by A. Simon and W.B. Thompson, Interscience Publishers, New York, 1969.

Holzer, T.E., J.A. Fedder and P.M. Banks, A comparison of kinetic and hydrodynamic models of an expanding ion-exosphere, J. Geophys. Res., 76,

2453-2468, 1971.

Hones, E.W., J. Birn, S.J. Bame, J.R. Ashbridge, G. Paschmann and N. Sckopke, Haerendel, Further determination of the characteristics of magnetospheric plasma vortices with ISEE 1 and 2, J. Geophys. Res., 86, 614-820, 1981.

Horwitz, J.L., C.R. Baugher, C.R. Chappell, E.G. Shelley and D.T. Young, Pancake pitch angle distributions in warm ions observed with ISEE 1, J. Geophys. Res., 86, 3311-3320, 1981.

Hovestadt, D., G. Gloeckler, C.Y. Fon, L.A. Fisk, F.M. Ipavich, B. Klecker, J.J. O'Gallagher and M. Scholer, Evidence for solar wind origin of energetic heavy ions in the earth's radiation belt, Geophys. Res. Lett., 5, 1055-1057, 1978.

Ince, E.L., Ordinary Differential Equations, Dover, New York, 1926.

Klimontovich, I.L., On the method of "Second Quantization" in phase space, Soviet Physics JETP, 6 (33), 753-760 (1958).

Krommes, J.A. and R.G. Kleva, Aspects of a renormalized weak plasma turbulence theory, Phys. Fluids, 22, 2168-2177, 1979.

Landau, L.D. and Lifshitz, E.M., Fluid Mechanics, Pergamon Press, New York, 1959.

Lemaire, J. and M. Scherer, Model of the polar ion-exosphere, Planet. Space Sci., 18, 103-120, 1970.

Lemaire, J. and M. Scherer, Simple model for an ion-exosphere in an open

magnetic field, Phys. Fluids, 14, 1683-1694, 1971.

Lemaire, J. and M. Scherer, Ion-exosphere with asymmetric velocity distribution, Phys. Fluids, 15, 760-766, 1972.

Lennartsson, W. and D.L. Reasoner, Low-energy observations at synchronous orbit, J. Geophys. Res., 83, 1103-1117, 1978.

Lundquist, S., Studies in magneto-hydrodynamics, Arkiv for Fysik, 5, 297, 1952.

Mange, P., The distribution of minor ions in electrostatic equilibrium in the high atmosphere, J. Geophys. Res., 65, 3833-3834, 1960.

Martin, P.C., E.D. Siggia and H.A. Rose, Statistical dynamics of classical systems, Phys. Rev., 8, 423-437, 1973.

Mishima, N., T.Y. Petrosky and R. Suzuki, Theory of irreversible processes in nonequilibrium quantum systems. I. General Formalism. J. Statistical Physics, 21, 347-392, 1979.

Misner, C.W., Thorne, K.S. and Wheeler, J.A., Gravitation, Freeman and Co, San Francisco, CA. 1973

Parish, J. L., Quantum Direct Interactions: The DIA of Turbulence Applied to a non-equilibrium quantum system, University of Iowa Research Report 79-4, 1979.

Pines, D., The Many Body Problem, Benjamin, New York, 1962.

Pines, D. and J.R. Schrieffer, Approach to equilibrium of electrons, plasmas and phonons in quantum and classical plasmas, Phys. Rev., 125, 804,

1962.

von Roos, Boltzmann-Vlasov equations for quantum plasma, Phys. Rev., 119, 1174-1179 (1960).

Rose, Harvey A., Renormalized kinetic theory of nonequilibrium many-particle classical systems, J. Statistical Physics, 20, 415-447, 1979.

Ross, J. and J.C. Kirkwood, The statistical-mechanical theory of transport processes. VIII. Quantum theory of transport in gases, J. Chem. Phys., 22, 1094-1103, 1954.

Saeng, A.W., Transport equation in quantum statistics for spinless molecules, Phys. Rev., 105, 546-558 (1957).

Schunk, R.W. and D.S. Watkins, Electron temperature anisotropy in the polar wind, J. Geophys. Res., 86, 91-102, 1981.

Schunk, R.W. and D.S. Watkins, Proton temperature anisotropy in the polar wind, J. Geophys. Res., 87, 171-180, 1982.

Semar, C.L. and A. Konradi, Field-aligned fluxes in the geomagnetic equator, J. Geophys. Res., 81, 1744-1750, 1976.

Sharp, R.D., R.G. Johnson, E.G. Shelley and K.K. Harris, Energetic  $O^+$  ions in the magnetosphere, J. Geophys. Res., 79, 1844-1850, 1974.

Shelley, E.G., R.G. Johnson and R.D. Sharp, Satellite observations of energetic heavy ions during a geomagnetic storm, J. Geophys. Res., 77, 6104-6112, 1972.

Shelley, E.G., R.D. Sharp and R.G. Johnson,  $He^{++}$  and  $He^+$  flux measurements

in the dayside cusp: Estimates of convection electric field, J. Geophys. Res., 81, 2363-2370, 1976.

Singh, N. and C.R. Baugher, Sheath effects on current collection by particle detectors with narrow acceptance angles, Space Science Instrumentation (in press), 1981.

Singh, N., W.J. Raitt and F. Yasuhara, Low energy ion distribution functions on a magnetically quiet day at geostationary altitude (L=7), in press J. Geophys. Res., 1981.

Sojka, J.J., W.J. Raitt and R.W. Schunk, Effect of displaced geomagnetic and geographic poles on high latitude plasma convection and ionospheric depletions, J. Geophys. Res., 84, 5943-5951, 1979.

Sojka, J.J., W.J. Raitt and R.W. Schunk, A theoretical study of the high-latitude winter F-region at solar minimum for low magnetic activity, J. Geophys. Res., 86, 609-621, 1981a.

Sojka, J.J., W.J. Raitt and R.W. Schunk, Plasma density features associated with strong convection in the winter high-latitude F-region, J. Geophys. Res., 86, 6908-6916, 1981b.

Takabayasi, T., The formulations of quantum mechanics in terms of ensemble in phase space, Prog. Theo. Phys., 11, 341-373 (1954).

Yeh, T., Kan, J.R. and Akasofu, S.-I., A Theoretically Derived Energy Coupling Function for the Magnetosphere, Planet Space Sci., 29, 425-429, 1981.

## 6. Figure Captions

- Figure 1. Electron distribution of counter-streaming electrons with streaming velocity of 10 eV and temperature of 4 eV versus momentum at first timestep.
- Figure 2. Electron distribution of counter-streaming electrons with streaming velocity of 10 eV and temperature of 4 eV versus momentum at timestep 19.
- Figure 3. Total electron density versus time.
- Figure 4. Plasmon distribution versus momentum at timestep 19.
- Figure 5. Plasmon density versus time.
- Figure 6. Plasmon damping decrement versus momentum at first timestep.
- Figure 7. Plasmon damping decrement versus momentum at timestep 19.

ORIGINAL PAGE IS  
OF POOR QUALITY

TIMESTEP 1.0

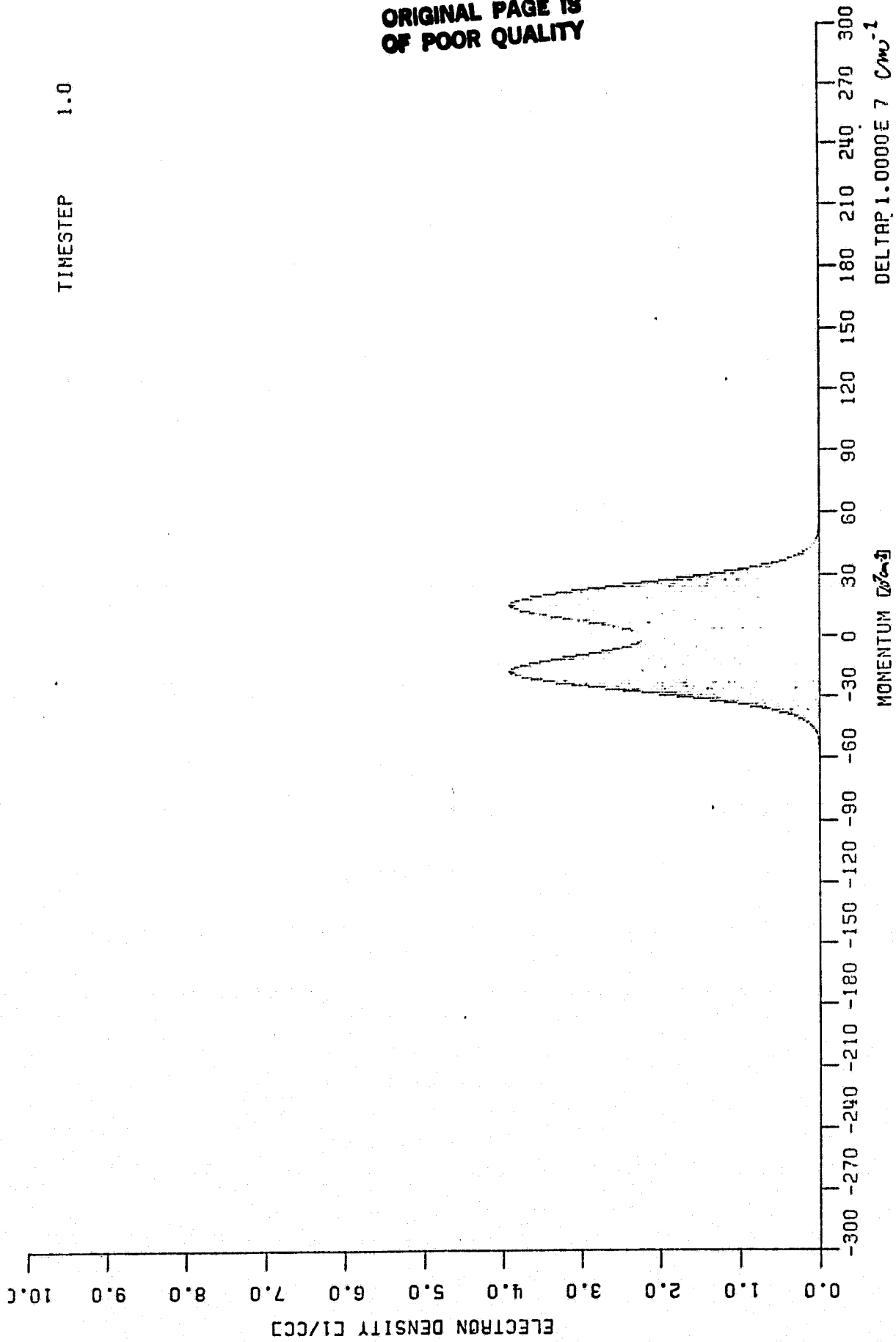


FIGURE 1

ORIGINAL PAGE IS  
OF POOR QUALITY

TIME STEP 19.0

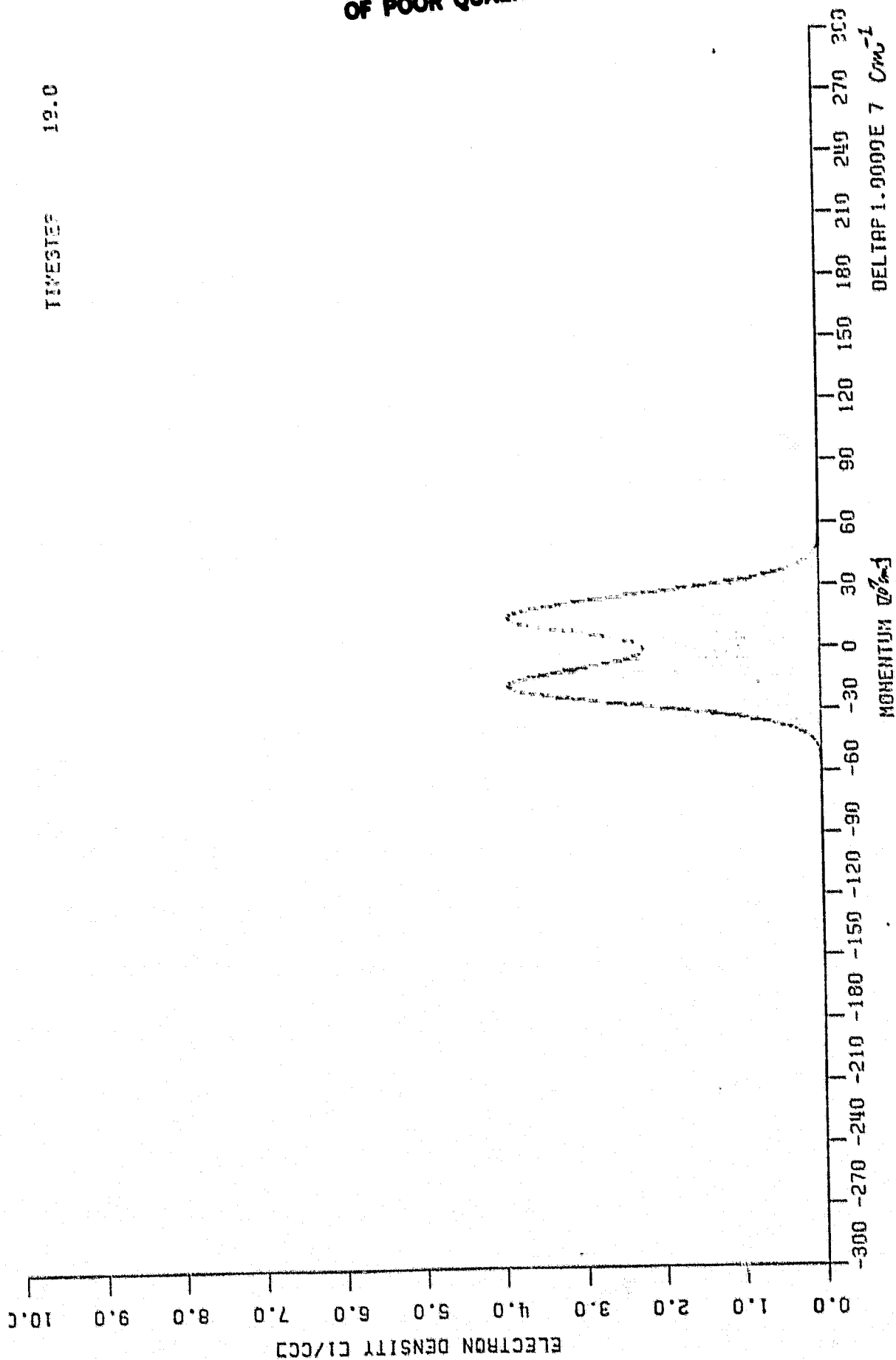


FIGURE 2



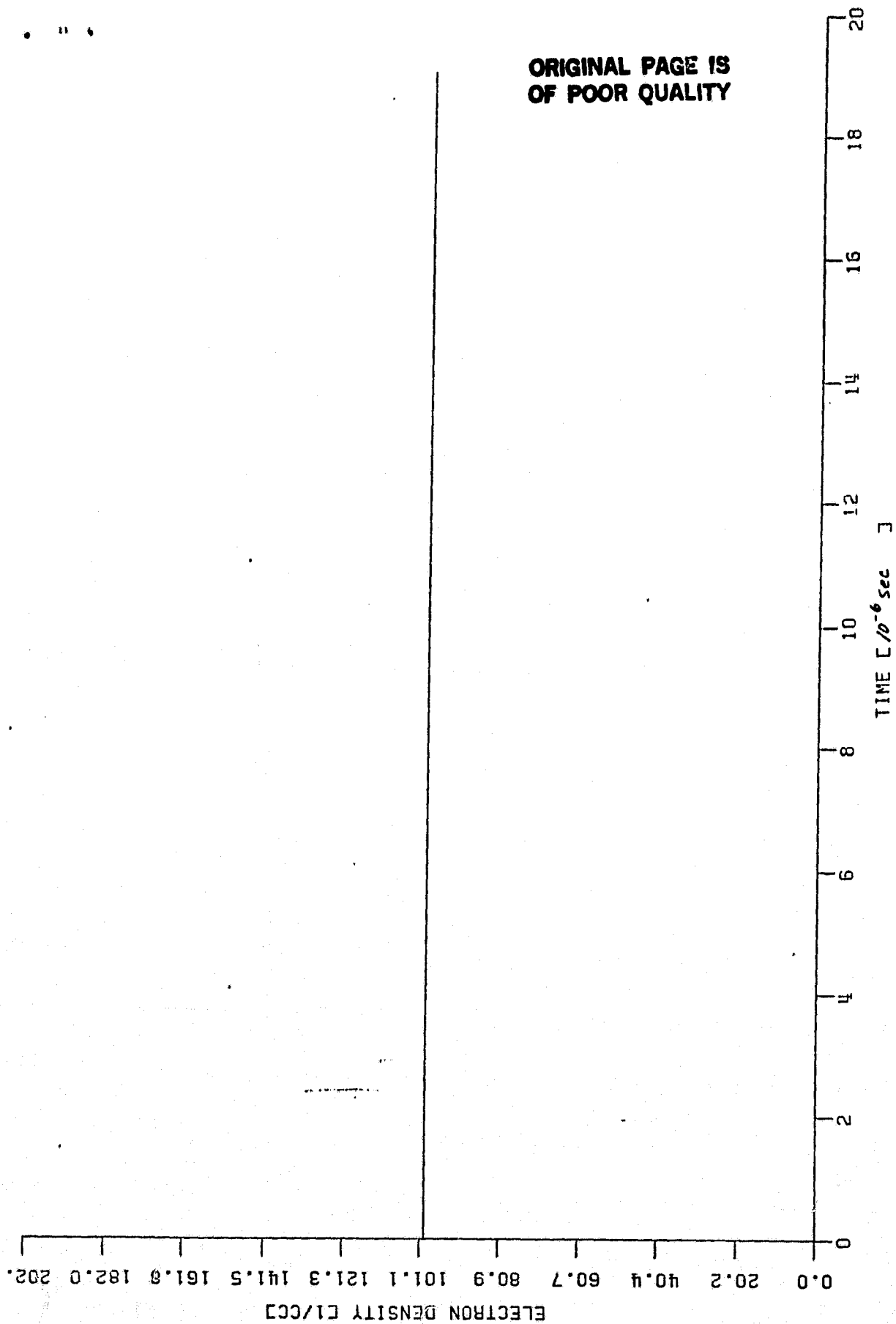


FIGURE 3

TIMESTEP 19.0

ORIGINAL PAGE IS  
OF POOR QUALITY

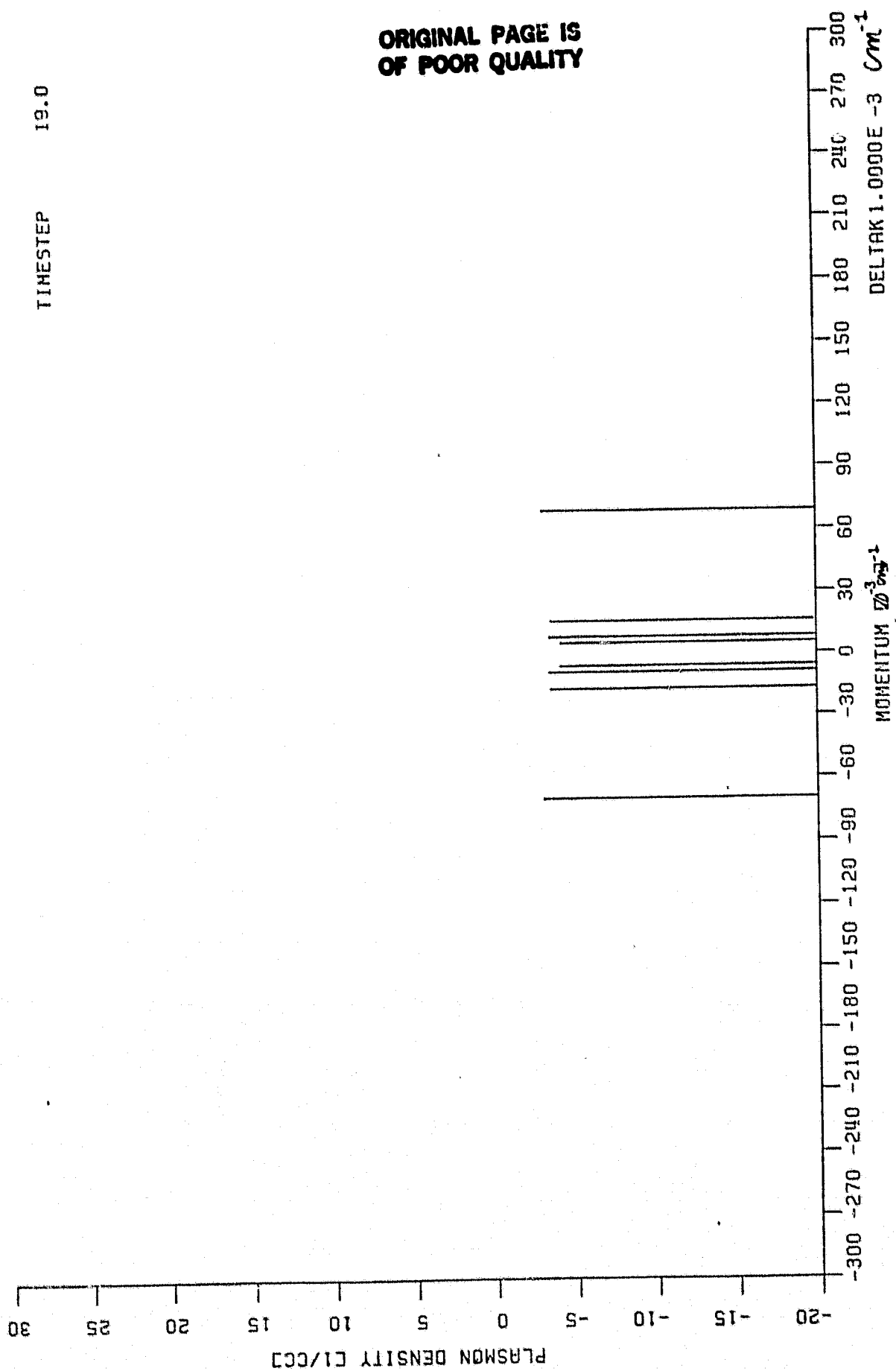


FIGURE 4

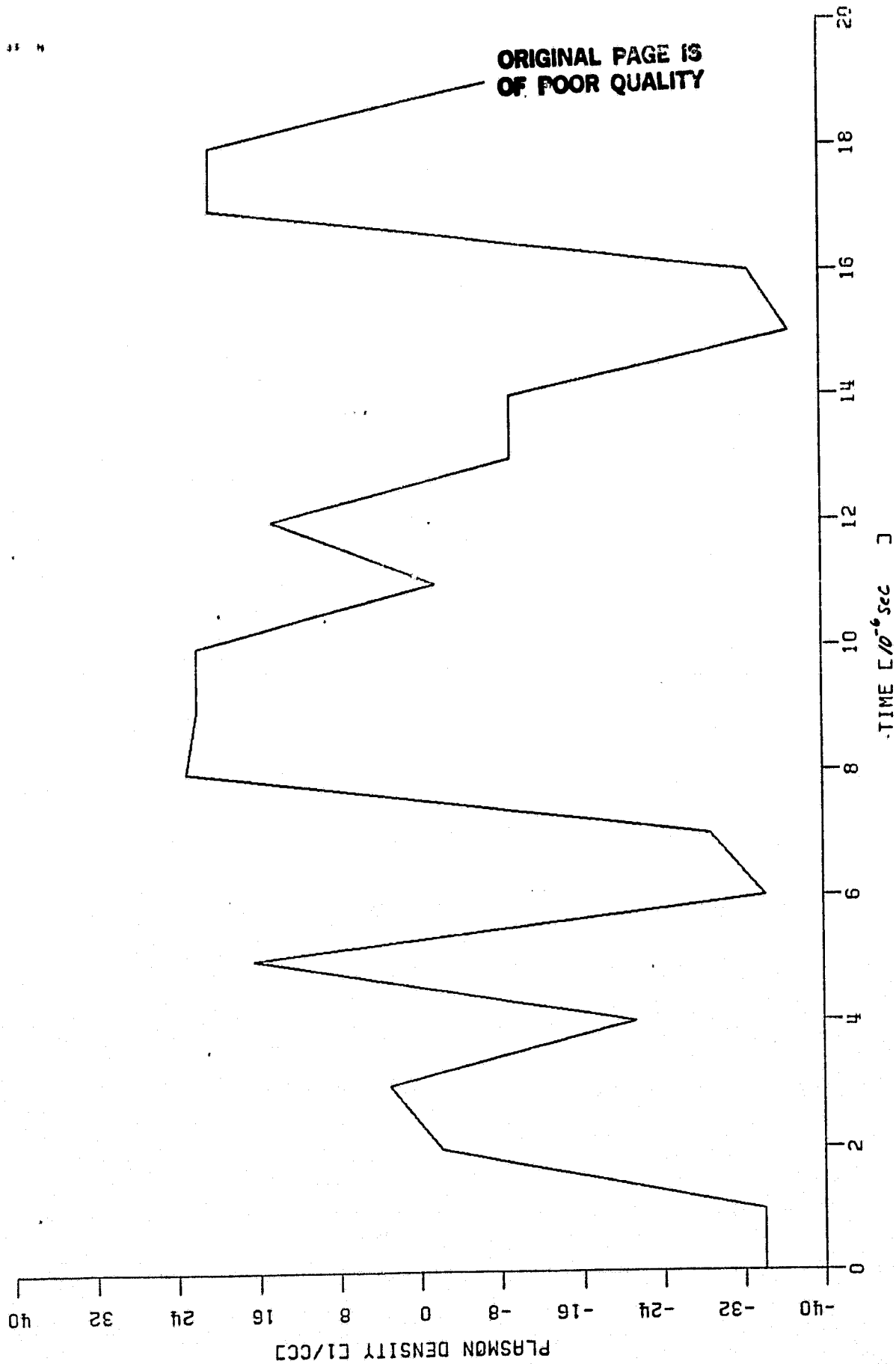


FIGURE 5

TIMESTEP . 1.0

ORIGINAL PAGE IS  
OF POOR QUALITY

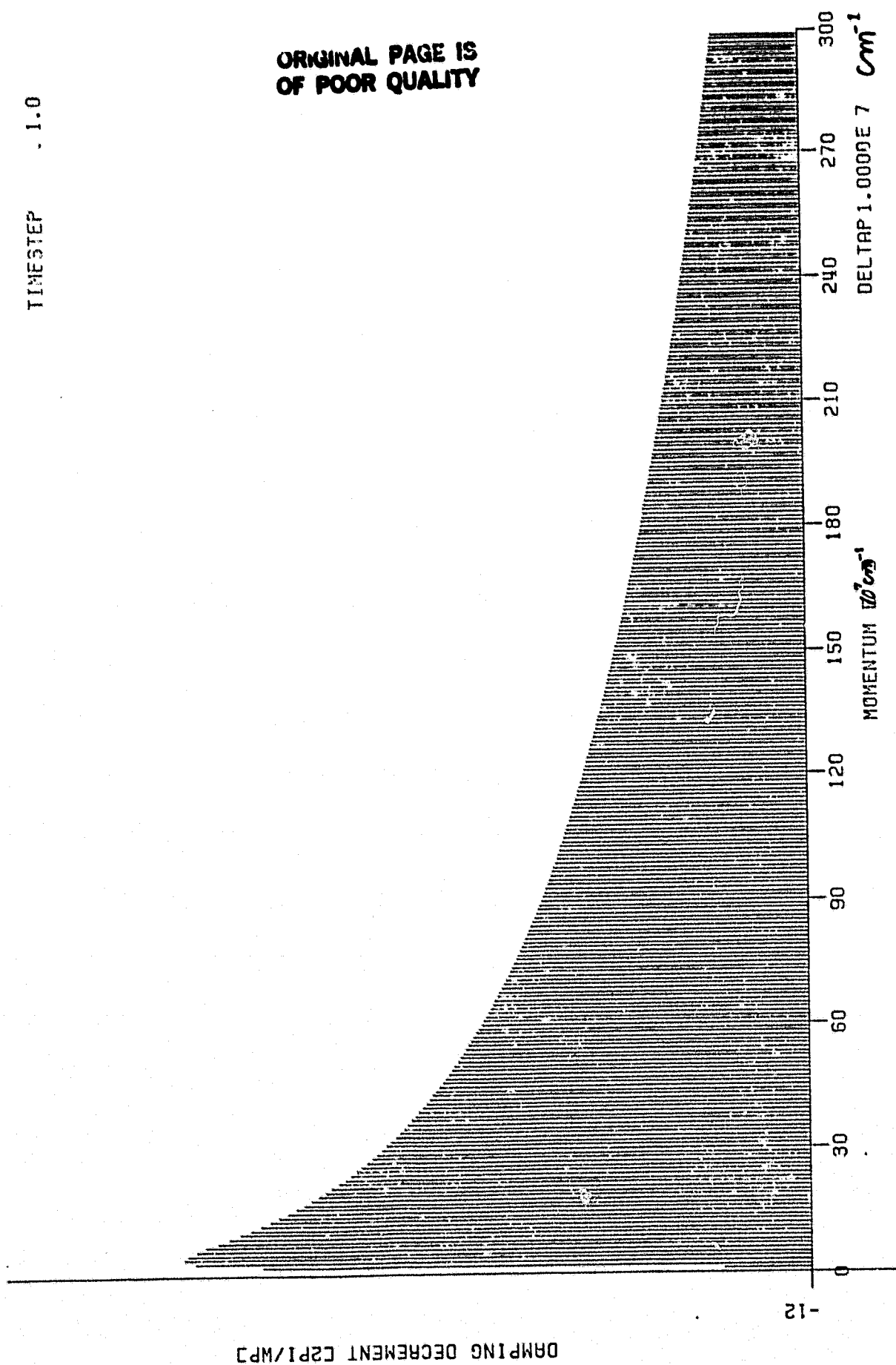


FIGURE 6

ORIGINAL PAGE IS  
OF POOR QUALITY

TIRESTEP 19.0

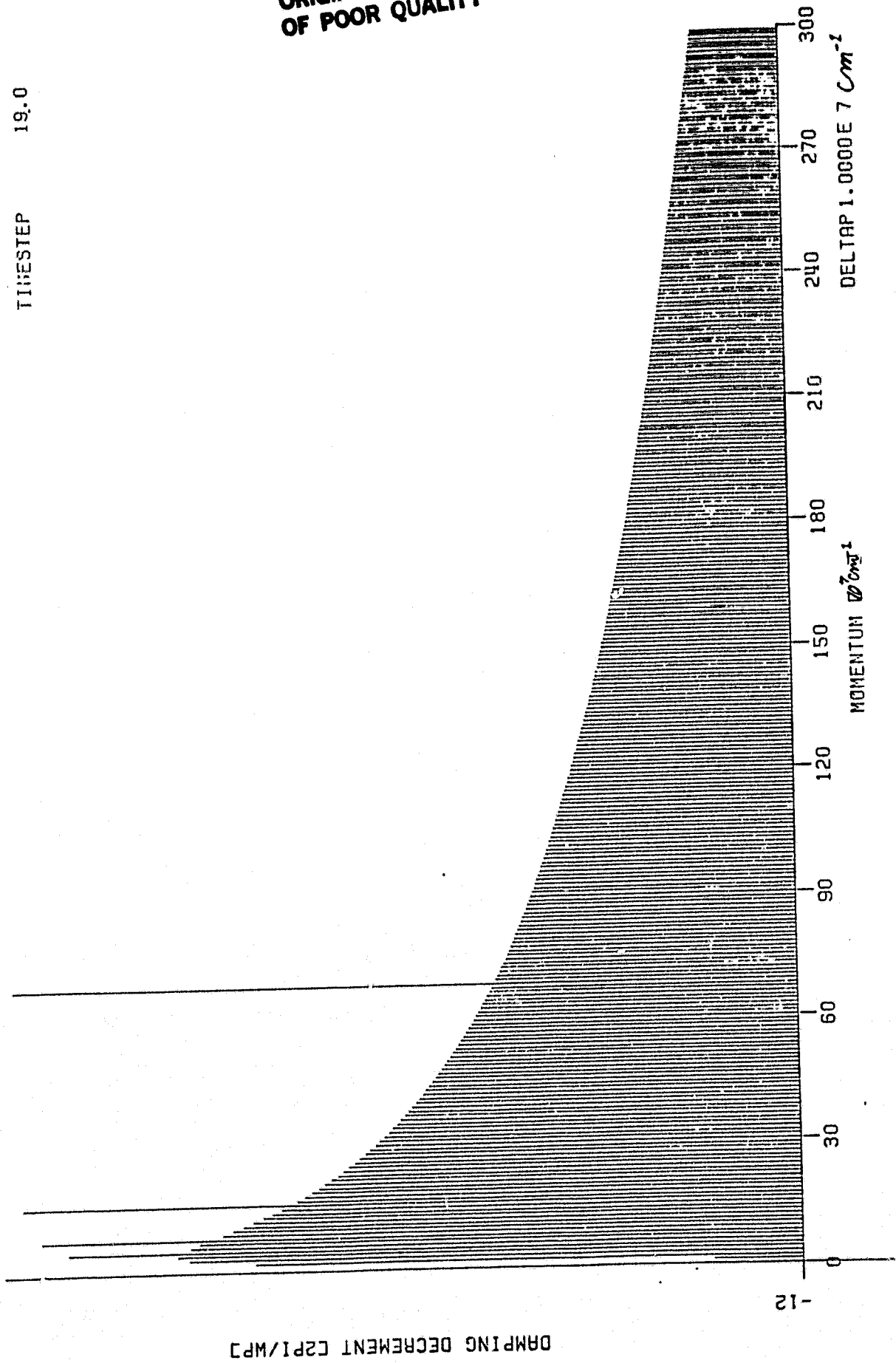


FIGURE 7